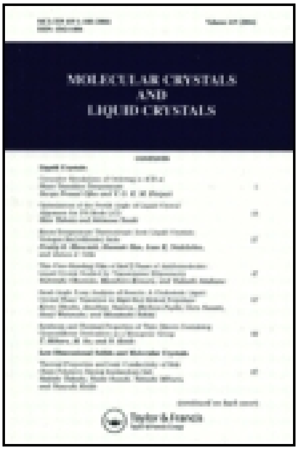

Molecular Crystals and Liquid Crystals

Publication details, including instructions for authors and subscription information:
http://www.tandfonline.com/loi/gmcl16

# Dynamic Light Scattering of Surface Fluctuations of a Nematic Liquid Crystal

L. B. Shih [a] , J. A. Mann [b] & G. H. Brown [c]

[a] Liquid Crystal Institute, Kent State University Kent, Ohio, 44242

[b] Corporate Research Division, S. C. Johnson & Son, Inc., Racine, Wl 53403

[c] Chemical Engineering Department, Case Western Reserve University, Cleveland, Ohio, 44106

Version of record first published: 17 Oct 2011.

To cite this article: L. B. Shih , J. A. Mann & G. H. Brown (1983): Dynamic Light Scattering of Surface Fluctuations of a Nematic Liquid Crystal, Molecular Crystals and Liquid Crystals, 98:1, 47-65

To link to this article: http://dx.doi.org/10.1080/00268948308073461

*Mol. Cryst. Liq. Cryst.*, 1983, Vol. 98, pp. 47–65
0026-8941/83/9804-0047/$18.50/0

Printed in the United States of America

# Dynamic Light Scattering of Surface Fluctuations of a Nematic Liquid Crystal

L. B. SHIH[†], J. A. MANN[‡] and G. H. BROWN[†]

*[†]Liquid Crystal Institute, Kent State University Kent, Ohio 44242, Current address of L. B. Shih: Corporate Research Division, S. C. Johnson & Son, Inc., Racine, WI 53403. [‡]Chemical Engineering Department, Case Western Reserve University, Cleveland, Ohio 44106*

*(Received May 27, 1983)*

The autocorrelation function of small amplitude capillary ripples was studied as a function of temperature for para-azoxyanisole (PAA). Measurements were carried out in the temperature range of 125°–148°C with the transition temperature observed to be 135°C. We will report our results for the case of $q = 252.0\ \mathrm{cm}^{-1}$. The spectra of the autocorrelation functions were fit by Lorentzian models to yield the surface tension as a function of temperature. Several "temperature jump" measurements were made wherein the current to the heaters was changed so that the equilibrium temperature at $T_0$ was perturbed slightly. Correlation functions were determined as the temperature increased to a new equilibrium state. Large shifts in frequency and time damping of the autocorrelation function were observed only when the temperature jump spanned the nematic-isotropic transition temperature. These results will be discussed. Equilibrium surface tension numbers are reported. The theory and practice for the light scattering measurement will be outlined briefly.

## INTRODUCTION

We report a series of measurements of the surface tension with temperature for para-azoxyanisole (PAA) using the grating method for resolving small angle, scattered light irradiance that is observed close to a laser beam reflected from the surface. Since the liquid crystal was in contact only with the walls of a relatively large Teflon container (ID = 3 cm), the free surface was in thermal and mechanical equilibrium consistent with the level to which we controlled temperature fluctuations. Our experiments involved a free surface area of about 7 $\mathrm{cm}^2$ and a laser beam diameter of about 0.2 cm that was incident on the center region of the free surface. We believe that this configuration minimized the possible orientational effects induced by the walls of the container on the liquid crystal sample.

We were motivated to make these measurements since theory[1] suggests a discontinuity in the surface tension at the temperature of the nematic-isotropic phase transition. Moreover, the experimental work reported in the literature for para-azoxyanisole (PAA) is equivocal on that point as well as being uncertain. The situation for PAA as well as other nematic liquid crystal systems has been reviewed thoroughly.[2] The conclusion was that the dynamic light scattering methods offer the possibility of eliminating the surface curvature effects and the wall effects on the molecular orientation that are intrinsic to each of the alternative methods.

Langevin and Bouchiat[3] and McQueen[17] have shown that quantitative light scattering measurements are possible from liquid crystal surfaces. They reported a measured fluctuation spectrum of PAA at only one temperature in the nematic phase. Moreover, the grating technology for resolving small wave number surface fluctuations was not developed at the time of their work. Work by several groups[4–6] have demonstrated the efficacy of the new grating technique. The work which we report was based on a first generation design[2,13] with the grating positioned in the optical path a few centimeters after the laser beam was reflected from the surface. We now know of more effective geometries.[4]

We anticipate that the work in progress in refining the grating technique for measuring the spectrum of light scattered by surface ripples will allow resolution of the balance of forces at the surface beyond the surface tension. The visco-elastic coefficients associated with surface ripple motion will be most interesting to study in liquid crystal systems. We limit this paper to an analysis of liquid crystal light scattering data[2] from which an estimate of the surface tension and the effective shear viscosity coefficient were computed as a function of temperature. Of special interest was the behavior of the ripple frequency at the transition temperature.

We will next describe the ripple structure and the instrument used to characterize the surface fluctuations. The results will be tabulated in a form which will allow the back-calculation of the original data, but we will use a dimensionless group representation. The trends in the data will be discussed with a special mention of the results of a temperature jump measurement made across the transition temperature.

## EXPERIMENTAL

### Description of surface wave dynamics

As a result of thermal fluctuations, the surface of the liquid crystal is covered by a cross-hatch of small amplitude capillary waves. These waves move in space and time according to the following function:

$$\zeta = \sum_{\mathbf{q}} \zeta_{\mathbf{q}}(t) e^{i\mathbf{q}\cdot\mathbf{x}}$$

where $\mathbf{q} = q\hat{e}$, $(q = 2\pi/\lambda_{\text{wave}})$, $\zeta_{\mathbf{q}}$ the time dependent amplitude of a capillary wave of wavelength $\lambda_{\text{wave}}$ and $\mathbf{x}$ a position on the surface. The space and time behavior of these waves can be modeled by continuum fluid mechanics since the characteristic wavelengths are always large compared to molecular sizes. It is also true that the amplitudes of the fluctuation-driven waves are small compared to wavelengths so that linearization of the fluid mechanical equations is valid. The fluid mechanical problem has been treated by numerous authors[7-10] and will not be repeated here. A boundary value problem is posed based on mass and momentum conservation in the volume of the fluid subject to boundary conditions that involve the surface response to fluctuations. The two key boundary equations follow:

$$0 = 2\gamma H - \hat{n}\cdot[\mathbf{P}]_{\Sigma}\cdot\hat{n} + \text{other terms} \tag{1a}$$

$$0 = \nabla\cdot\overline{\boldsymbol{\sigma}} - \hat{n}\cdot[\mathbf{P}]_{\Sigma}\cdot\mathbf{U}_{\hat{n}} \tag{1b}$$

where $\gamma$ is the surface tension, $H$ is the mean radius of curvature and is $(-\frac{1}{2}(\partial^2\zeta/\partial x^2))$ for small amplitude, cylinder waves propagating along the $x$-direction, $\hat{n}$ the normal to the surface and $[\mathbf{P}]_{\Sigma}$ the jump of the pressure tensor across the surface. Other terms may be added to Eq. (1a) that take into account bending viscoelastic effects in the interface. Such terms will be ignored in the analysis of our results. Moreover, following Langevin *et al.*,[3] we ignore liquid crystal elastic coefficients in the analysis of our data.

Equation (1b) represents the in-plane motion of the surface where $\overline{\boldsymbol{\sigma}}$ is the two dimensional stress tensor and $\hat{n}\cdot[\mathbf{P}]_{\Sigma}\cdot\mathbf{U}_{\hat{n}}$ is the projection onto the surface of the pressure tensor jump across the surface. The special characteristics of liquid crystals at the interface come into the character of the surface stress tensor $\overline{\boldsymbol{\sigma}}$, as well as in the extension of Laplace's equation to include bending modes. The bulk phase properties of liquid crystals come in as part of the pressure tensor that is used to compute the jump terms. A complete description of the dynamics would also involve the director. The work of Langevin and Bouchiat[3] suggests that the simplification of the boundary value problem to that for which $\nabla\cdot\overline{\boldsymbol{\sigma}} = 0$ will be sufficient until such time as we can measure the characteristic frequencies of the waves to between 0.01% and 0.1%. We believe that this level of precision and accuracy will be realized eventually.

The solution of the boundary value problem using the classical initial conditions leads easily to the following dispersion relationship[11]

$$0 = (1 + s)^2 + Y - \sqrt{1 + 2s} \tag{2}$$

where $s$ is the dimensionless frequency which in our case (propagating ripples) is complex with

$$s = -\frac{\Gamma}{\Gamma_0} + i\frac{\omega}{\Gamma_0} \quad \text{and} \quad Y = \left(\frac{\omega_0}{\Gamma_0}\right)^2 .$$

The variables

$$\omega_0 = \sqrt{\frac{\gamma q^3}{\rho}} \quad \text{and} \quad \Gamma_0 = 2\frac{\mu}{\rho}q^2$$

are the frequency for waves traveling on an ideal liquid and the time damping of waves following potential flow kinematics on a real liquid. The two variables $\mu$ and $\rho$ are the shear viscosity and the density of the liquid. The variables $\omega$ and $\Gamma$ are the frequency and time damping coefficient for surface ripples of wave number $q$ and are to be determined by analysis of the correlation function of the intensity of scattered light.

This dispersion relationship can be reorganized into a form with dimensionless groups defined as follows

$$Y_1^{-1} = \left(\frac{\omega_0}{\omega}\right)^2 = \frac{\gamma q^3}{\rho\omega^2}, \qquad Y_2 = \frac{\Gamma}{\omega}, \quad \text{and} \quad Y_2^\circ = \frac{\Gamma_0}{\omega} \tag{3}$$

so that Eq. (2) becomes

$$0 = (\hat{Y}_2 + Y_2^\circ)^2 + Y_1^{-1} - (Y_2^\circ)^{3/2}\sqrt[+]{Y_2^\circ + 2\hat{Y}_2} \tag{4}$$

where $\hat{Y}_2 = Y_2 + i$. $Y_1$ and $Y_2$ were first defined by Hansen and Mann[18] for the space damping description of forced capillary wave motion. These are the dispersion relationships (Eqs. 2 and 4) that we have used in our analysis of the data. As is apparent from Eq. (4), only the ratio represented by $Y_2$ is required for determining $Y_1$ (and thereby $\gamma$) and $Y_2^\circ$ (and thereby $\mu$).

Langevin and Bouchiat[3] have developed a more complicated dispersion relation based on a constitutive equation for the pressure tensor, **P**, that involves three viscosity coefficients $\eta_1$, $\eta_2$ and $\eta_3$. For a normal fluid $\eta_1 = \eta_2 = \mu$ and $\eta_3 = 0$. The coefficients are related in a complicated way with the Leslie parameters.[3] We generalized their model to include the possibility that the surface, under our experimental conditions (no magnetic fields), was not well ordered so that the distribution function for the director was assumed uniform. The resulting dispersion relation was identical in form to theirs except that $\Gamma_0$ involved both $\eta_1$ and $\eta_2$, and their ratio $\eta_3/\eta_1$ was weighted by the expectation value $\langle(\mathbf{q} \cdot \hat{n})^2\rangle$ where $\hat{n}$ is the director. This equation involves three parameters, $\omega_0$, $\Gamma_0$ and the ratio $\eta_3/\eta_1$. With $q$ fixed, only two parameters can be determined.

Our experiments were run under conditions for which there appears to be little to discriminate between Eq. (2) with $\mu$ taken to be an effective viscosity coefficient and the more general relationship.[3] The focus of this paper is the computation of the surface tension which can be done adequately with Eq. (4) and not the viscosity coefficients. We expect to study the more general dispersion relation in the future.

The value of $Y$ allows the overdamped regime to be distinguished from the propagating wave regime for these simple dispersion equations. In our experiments the dimensionless group, $Y$, was always significantly greater than 1. In this regime[4,13] the autocorrelation function of the Fourier components of the surface elevation can be written directly as

$$R_q(\tau) = \langle \zeta_q^*(0)\zeta_q(\tau)\rangle = \frac{k_BT}{A(\gamma q^2 + \Delta\rho g)} e^{-\Gamma\tau} \cos \omega\tau \tag{5}$$

where $A$ is the surface area, $T$ is the temperature, $k_B$ is the Boltzmann constant, and $\Delta\rho$ is the density difference of the two phases and is the density of the liquid phase in our study while $g$ is the gravity constant. The experimental method is based on determining $\Gamma$ and $\omega$ with $q$ and the density, $\rho$, known. The dispersion relationship then allows the calculation of $Y_1$ and $Y_2^\circ$. The surface tension is then calculated from the definition of $Y_1$ and the effective viscosity from $Y_2^\circ$ and their numerical values as determined through finding solutions consistent with the dispersion relationship, Eq. (4). This correlation function can be measured by light scattering methods.

The small amplitude capillary waves that cover the interface behave as a dynamic grating. The reflectivity of the surface is given by

$$R = r_0(1 + \eta)e^{i\phi} \tag{6}$$

where $r_0$ is the reflectivity of the smooth surface, $\eta = \eta(\mathbf{x})$ represents the variation in reflectivity over the surface and $\phi = 2k_0\zeta(\mathbf{x}, t)$ the phase function. The number $k_0$ is $2\pi/\lambda_0$, where $\lambda_0$ is the wavelength of the incident beam. We assumed that $\eta \ll 1$ so that the ripples act as a phase grating. The experimental method then is to project a grating stationary in time and in space onto the surface so that a superposition of the effect of the phase grating that is the rippled surface and the projection is detected in the far field. Application of the methods of Fourier Transform Optics[4] show that, if the various grating orders are sampled individually by a pin-hole mask located in the far field, Figure 1b, and the correlation function computed for the photocurrent, the result will be

$$R_{k_e}(\tau) = \langle i(0)i(\tau)\rangle_{k_e} = Ae^{-\Gamma_{k_e}\tau} \cos \omega_{k_e}\tau + B + C\delta(\tau) \tag{7}$$

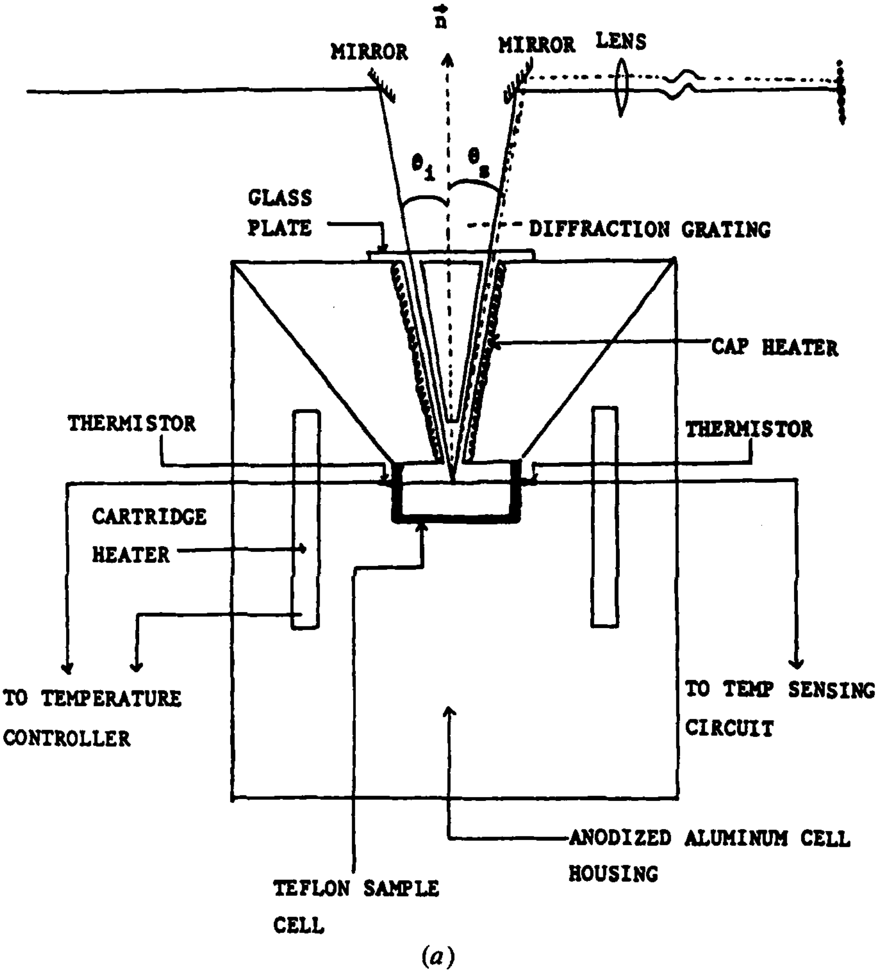

FIGURE 1a Cross-sectional view of the temperature-regulated sample cell and its housing.

to a good approximation, where $i$ is the photocurrent output from the detector. Thus, the optical components and electronic components of the apparatus are designed so as to give a photocurrent correlation function that has the form of Eq. (5). Here $k_e$ is the effective grating constant at the surface. While $\omega_{k_e}$ is nearly $\omega_q$, there can be instrumental broadening of $\Gamma_{k_e}$; $\Gamma_{k_e} \neq \Gamma_q$ in general. Further, it is important to calculate the actual wave number being sampled, $q$. Only for an ideal optical system will $k_e = q$ hold. See Edwards *et al.*[4] for a discussion of this point. This is crucial since

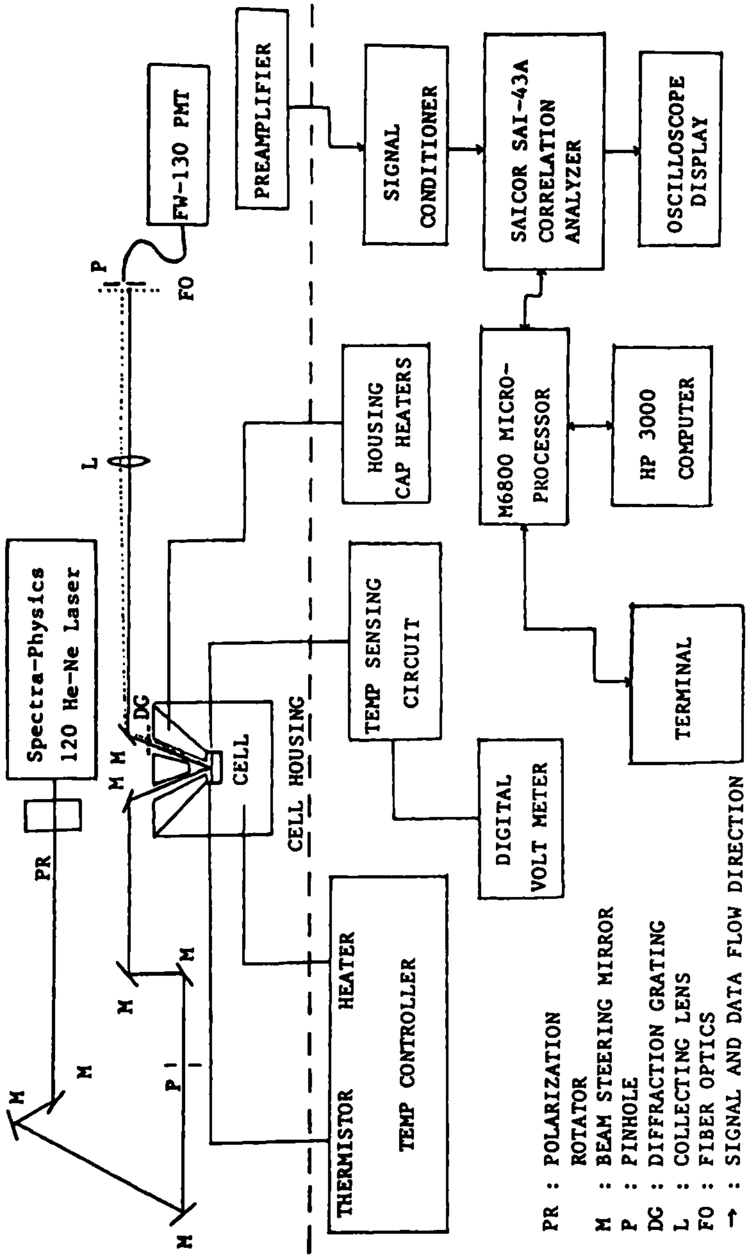

FIGURE 1b Block diagram of experimental setup of surface scattering apparatus.

an error of 1% in estimating $q$ means a 3% error in the surface tension. In most practical optical systems both $\Gamma$ and $\omega$ must be corrected for the finite diameter of the illuminated spot on the surface and there must be a correction for the propagation properties of a beam of Gaussian cross section through the optical elements. The correction computed for $\Gamma_{k_e}$ was about 20% of the measured value, for $k_e$ it was about 1% whereas the correction for $\omega_{k_e}$ was small enough to ignore. The details of these corrections are to be found in the papers of Hård,[5] Shih[2] and, more recently, Edwards, *et al.*[4]

## Description of the light scattering spectrometer

The experimental apparatus[2] is shown schematically in Figure 1. The temperature regulated sample compartment was made from a solid piece of aluminum with a diameter of 11.4 cm and a height of 13.3 cm. The sample container was made of Teflon machined to an inside dimension of 3 cm and a height of 1.5 cm and was tightly fitted into the center of the housing. The aluminum housing was black anodized and the outside covered with a 1 in. thick coating of insulating materials. Six cartridge heaters, each which had a power or 80 watts at 120 volts, were implanted in the housing. Thermistors were used to monitor the temperature of the sample cell as well as to generate a signal for the temperature control circuit. The control circuit could keep the temperature fluctuations to within 0.01°C, but resetability was only to within 0.1°C. The sample compartment was mounted on an x-y-z translator and a polar rotator that rotated in the plane of the sample surface.

Holes of 1.9 cm in diameter were drilled in the cap to allow the laser beam to enter and to exit. The incident and reflection angles were 10° from the surface normal for these studies. In order to compensate for the heat loss from the openings for the beams, two separate heaters were placed in the housing cap. The heaters could be manually adjusted to compensate for the heat loss. The original design called for optical quality glass plate to cap the Teflon sample cell, Figure 1a. This proved to be impractical since the window fogged up excessively from PAA vapor. Instead, a glass plate, shown in Figure 1a, closed off the two ports for the incident, reflected and scattered beams.

Teflon was used for the sample container since it is chemically stable at elevated temperatures and PAA doesn't wet the polymer completely. The design of the Teflon cell was such that a flat surface could be obtained at the center of the cell. This is a critical part of the experiment. Even a very small curvature in the surface will distort the value of the grating constant $k_e$ that one would expect from the projection of the grating back on to the surface.[2,4] In a subsequent experiment we measured the flatness of the liquid surface of PAA in the cell that was used in this study and found that the radius of curvature was of the order of 2 m. We showed that the radius of curvature remained constant throughout the entire temperature range studied. This effect was ignored as being small compared to other uncertainties. Had the radius of curvature been much smaller than this (~1 m) a noticeable systematic distortion of the apparent wave number of the fluctuations would have been evident. Knowing accurately the wave number, $q$, of the surface ripplons that are sampled by the grating still remains a problem for the light scattering methodology.[4,13]

The detection and the subsequent calculation of the intensity autocorrelation function has been well described in other publications.[2,3,6,13]

A typical correlation function collected with the apparatus used for this study is shown in Figure 2a. A nonlinear least squares procedure using Eq. (7) can be used to extract the center frequency, $\omega_{k_e}$, and spectral width, $\Gamma_{k_e}$, that are then used in a further reduction procedure. We[2] performed a Fast Fourier Digital Transformation on the correlation function data in order

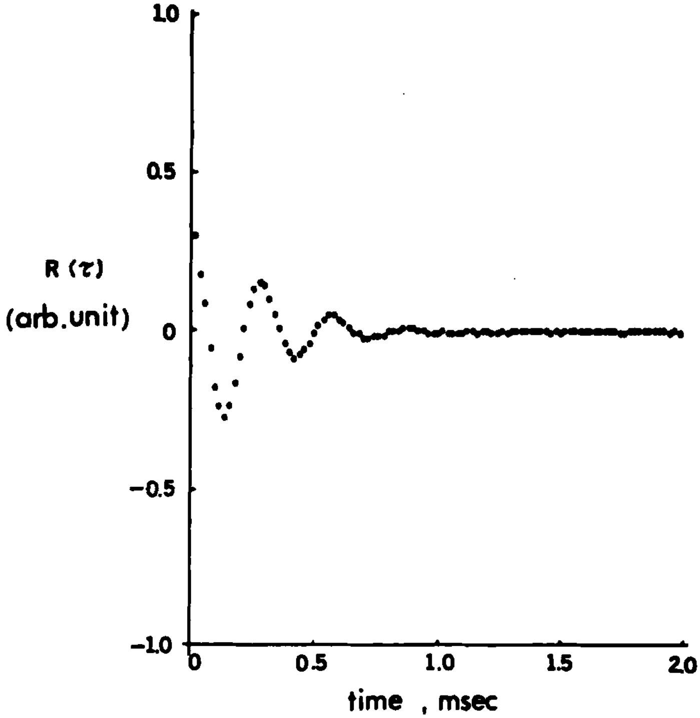

FIGURE 2a 100 point autocorrelation function, PAA at $T$ = 131.5°C and $k_e$ = 252 cm$^{-1}$. The function was normalized to bin 0 which corresponds to $\tau$ = 0.

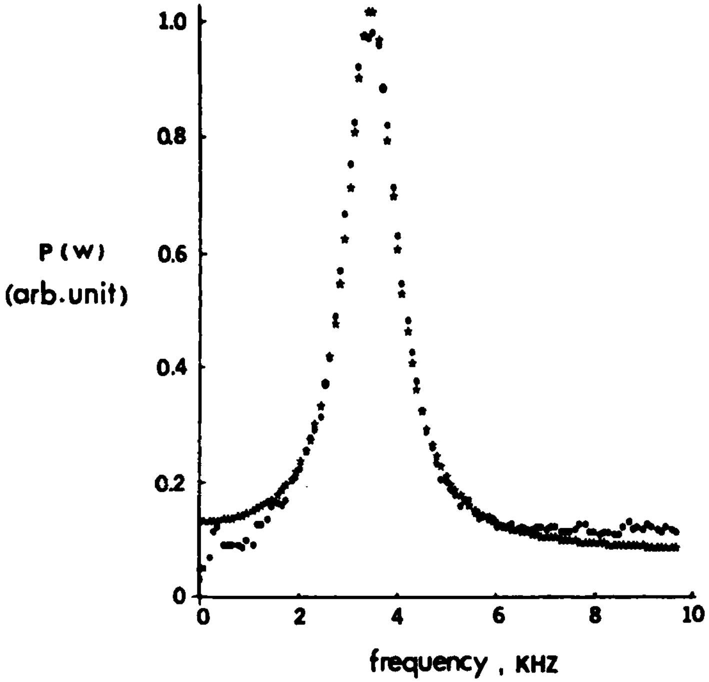

FIGURE 2b The plot of the least-square fit results for the data set for $T = 131.5°C$ and $k_e = 252\ \text{cm}^{-1}$, the FFT of Figure 2a.

to curve-fit the spectrum. Care must be taken to correct for the small errors induced by the FFT algorithm. Lorentzian line shape functions were used for the fits which provided the center frequency, $\omega_{k_e}$, and the half width at half height information, $\Gamma_{k_e}$, needed for further processing. We found that processing the original correlation data[12] using Eq. (7) in a weighted nonlinear least squares procedure gives sensibly the same result as obtained from the curve-fit in the frequency domain. The spectrum analysis is preferred when the correlation function is noisy.[2,13]

About 20% of the measured spectral width was due to instrumental broadening effects. Our[2,4,13] analysis of the scattered light spectrum of ethanol as a function of $q$ demonstrated that the correction can be computed accurately. In particular when the dimensionless groups $N = k_e\sigma_{\text{surg}} > 10$ and $NY_2 > 2$ ($\sigma_{\text{surf}}$ is defined after Eq. 8) hold the correlation function will have the form of Eq. (7). For our liquid crystal work $N = 14.4$ and $NY_2 = 2.26$ so that we could use the algorithm of Hård[5] in computing this correction. An iteration scheme must be used that involves the surface tension itself as follows

$$\Gamma_q \cong \Gamma_{k_e} - \frac{\Gamma_l^2}{\Gamma_{k_e}} \tag{8}$$

where

$$\Gamma_l = c\frac{\cos^2 \theta_l}{8\sigma_{\text{surf}}}\sqrt{\frac{\gamma q}{\rho}}$$

$c = 10$ if the frequencies are in radians/s and 1.59 if in Hz, $\theta_l$ the incident angle, and $\sigma_{\text{surf}}$ the standard deviation of the Gaussian cross section of the beam at the surface. The Gaussian cross section was measured directly by scanning the beam at the location of the surface with a moving pin-hole of a few micrometers in diameter backed by a photo-current detector.

Clearly an estimate of $\gamma$ is required in order to use Eq. (8). The initial estimate of $\gamma$ was done by assuming $Y_1^{-1} = 1$, Equation (3). Refinements were made using the dispersion relationship, Eq. 2 or 4 to calculate new estimates of $\gamma$. The sequence was as follows. We[2,13] used the imaginary part of the dispersion relationship, Eq. (2), that had been rationalized in order to provide a computation of the shear viscosity, $\mu$, of the fluid as the root of a sixth degree polynomial in $\mu$. The result of this computation was used in an expression[2,13] for the surface tension that was derived from the real part of the dispersion relationship, Eq. (2). Once the new estimate of $\Gamma_q$ had been calculated, Eq. (8), that number along with $\omega$ was used to compute $\mu$ and $\gamma$. The estimate of the surface tension, $\gamma$, was used to compute a new $\Gamma_q$, etc. Between three and seven iterations were required for the process to converge so that the change in $\Gamma_q$ was less than 0.001%.

It was obvious that the polynominal representation[2,13] for the viscosity had a number of real roots. We found that if the initial estimate of the viscosity is low by even 2% the procedure will converge to a nonphysical root. If the estimate of $\mu$ that is used to initiate the procedure is larger than the root (even by factors of 10), the proper root is always computed. As we have mentioned, once the $\mu$ number is computed, a direct calculation gives an estimate of the surface tension.

Becuase of the root difficulty[11] with the direct calculation of $\mu$, a new program was written based on the dispersion relationship as shown in Eq. (4) which did not involve rationalization of the dispersion equation. The program always converged to numbers that were consistent with the dispersion equation, Eq. (2). Each number we report herein has been checked to be sure that it is consistent with the dispersion relationship, Eq. (2) or (4).

We[2,13] showed that this procedure produced an accurate representation of the capillary ripple dispersion on the ethanol surface. There is a gratifying correspondence between theory and experiment that has been missing in work reported by previous investigators.[14] The work[2,13] verified that in the scattering geometry used for the liquid crystal studies the effective wave number, $k_c \approx q$, could be taken as 252 $\text{cm}^{-1}$.

### Materials

The PAA was purchased from various sources: Aldrich Chemical, Eastman Kodak Co. and Frinton Laboratories. The samples used in this study were purified by recrystallization from 100% ethanol. After recrystallization, the compound was dried in a vacuum oven at 40°C for 8 h and then kept in a refrigerator until used. The purity of the sample was verified by IR and NMR spectroscopic measurements.

A new sample was used for each run during which the temperature ranged from 125°C to 145°C during an 8 to 12 h period. During the measurements, the sample surface was cleaned from time to time by using a heated micropipet connected to a clean, vacuum source. After the surface was suctioned, about 10 min was allowed for thermal equilibrium to be reestablished before recording additional correlation functions. While the surface cleaning procedure changed the level of the liquid surface slightly, this change was small and the effect ignorable in analyzing the data.

PAA was selected for study[2] because there were reliable density and viscosity measurements in the literature. There were preliminary light scattering measurements reported by two groups.[3,17] Further, measurements of the anisotropy of surface reflectivity to polarized light[19] showed that at the surface, the director is parallel to the surface.

## RESULTS

Table I consists of the results of the measurements of the fluctuation spectra of PAA over a temperature range that includes the transition temperature from the nematic phase to the isotropic phase. Figure 2 shows a typical example of a correlation function and its FFT. The spectra for the temperature jump experiments showed a poorer signal to noise ratio since the averaging time for collecting each correlation function was reduced. The variation with temperature of the center frequency and the half-height-half-width frequency as determined by fitting the spectra with Lorentzian functions[2] are reported. Both uncorrected and corrected spectral widths are reported.

The propagation of the uncertainty[7] in the spectral width numbers to uncertainties in the surface tension is relatively small. These errors are far more important for the estimation of the viscosity, $\mu$. It is clear from Table I

TABLE I

Capillary wave parameters for PAA as a function of temperature

| $T$ °C | $f_0$ Hz | $Y_1$ | $1/y_1$ | $f'^*$ Hz | $f'$ Hz | $Y_2^\circ$ | $Y_2$ |
|---|---|---|---|---|---|---|---|
| 128.1 | 3437 | .928 | 1.078 | 627 | 501 | .188 | .146 |
| 129.9 | 3452 | .939 | 1.065 | 608 | 455 | .167 | .132 |
| 131.5 | 3446 | .941 | 1.062 | 596 | 442 | .161 | .128 |
| 132.3 | 3458 | .914 | 1.094 | 702 | 564 | .214 | .163 |
| 132.8 | 3458 | .900 | 1.111 | 752 | 623 | .241 | .180 |
| 134.7 | 3354 | .918 | 1.089 | 665 | 531 | .206 | .158 |
| 134.9 | 3535 | .911 | 1.097 | 727 | 589 | .220 | .167 |
| 134.9** | 3936 | .911 | 1.098 | 811 | 658 | .220 | .167 |
| 134.9** | 4345 | .870 | 1.149 | 1074 | 926 | .296 | .213 |
| 134.9** | 4684 | .901 | 1.110 | 1014 | 839 | .240 | .179 |
| 136.1 | 3326 | .897 | 1.115 | 734 | 611 | .247 | .184 |
| 139.2 | 3429 | .932 | 1.073 | 631 | 485 | .181 | .141 |
| 144.0 | 3488 | .910 | 1.099 | 713 | 588 | .223 | .169 |
| 148.3 | 3468 | .921 | 1.086 | 680 | 540 | .202 | .156 |

*Uncorrected for instrumental effect, see text.

**First: 'equilibrium' conditions but very close to transition.

**Next two: 'temperature jump' of about 0.2°C. $k_e = 252\ \mathrm{cm}^{-1}$, $\Gamma_{k_e} = 2\pi f'^*$, $\Gamma_q = 2\pi f'$

that a correction that often amounts to 20% of the width must be applied as due to the instrumental function for the optical configuration used for the measurements. Even though Hård, *et al.*[5] and Edwards, *et al.*[4] have developed theories for correcting $\Gamma_{k_e}$, it is difficult at this time to estimate the accuracy with which we can compute the correction. Based on our experimental work with ethanol,[2,13] and the nonlinear least squares estimation of fitting errors we believe that the uncertainty of determining $\Gamma_q$ to be about 5%.

We are much more certain about the center frequencies reported in this table. The major error in the center frequency would be due to the uncertainty in $k_e$. The grating and the optical system were well characterized in the experiments on ethanol[2,13] in which the surface area was large enough that there was little question about its flatness. Our best estimate of $q$ is 252 ±1.5 cm$^{-1}$. There remains the question as to whether the liquid crystal interface was sufficiently flat that the projected grating on the surface would have the same $k_e$ as the ethanol experiments. We can say that the surface curvature did not change in the temperature region around the transition temperature. Our best estimate is that the uncertainty in the $k_e$ due to the surface curvature results in an uncertainty of no more than 20 Hz in the center frequency.

The density of PAA was taken from the measurements of Chatelain.[15] His data were fit by a polynomial over the range of 105° through 137°C. The data are sufficiently smooth that a polynomial of the third degree gave a sufficiently accurate interpolation and extrapolation for the temperatures covered in our study.

The center frequency data are plotted as a function of temperature in Figure 3. The data recorded at the transition temperature, which is a fraction above 134°C, showed a rapid change. (This temperature was as close to the phase transition temperature as we could set our controller.) The large change in center frequency that we observed slightly above 134.9°C was a surprise. The temperature of the cell was set to 134.9°C and, once equilibrium had been attained, the power input to the cell housing was changed slightly. The temperature then increased very slowly by 0.2 of a degree through the transition temperature. The heating rate was slow compared to the rate at which we could compute correlation functions. The result of such a temperature jump experiment is reported in Figure 3 as the starred points. The apparent ripple frequencies recorded during the temperature jump increased far beyond that which we had expected. Due to limitations in the control of the temperature and the rate-of-change of temperature, the frequencies observed in the transition region were not quantitatively repeatable.

Effective viscosity numbers can be calculated from Tables I and II by recognizing that

$$\mu_{\text{eff}} = \frac{\rho\omega}{2q^2} Y_2^\circ$$

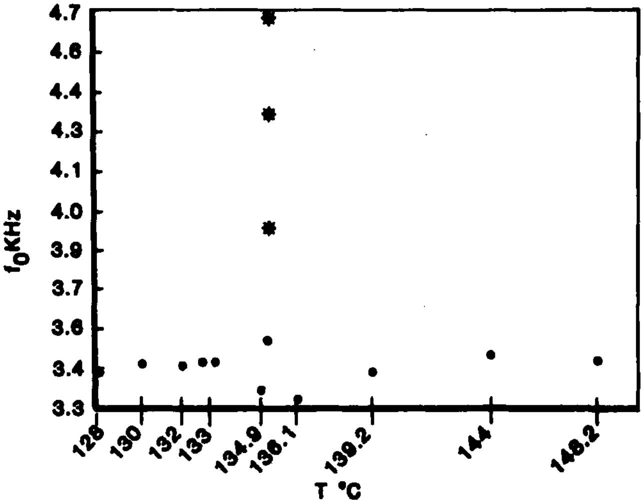

FIGURE 3 Center frequency vs $T$ for PAA. $k_e = 252\ \text{cm}^{-1}$.

TABLE II

Surface Tension with Temperature

| $T$ °C | $1/y_1^{**}$ | $f_0$ Hz | $\rho$ gm/cm$^3$ | $\gamma$ d/cm |
|---|---|---|---|---|
| 128.1 | 1.07 | 3437 | 1.159 | 36.1 |
| 129.9 | 1.08 | 3452 | 1.157 | 36.7 |
| 131.5 | 1.09 | 3446 | 1.155 | 36.9 |
| 132.3 | 1.095 | 3458 | 1.155 | 37.3 |
| 132.8 | 1.097 | 3458 | 1.154 | 37.3 |
| 134.7 | 1.10 | 3354 | 1.149 | 35.1 |
| 134.9 | 1.10 | 3535 | 1.149 | 39.0 |
| 134.9* | 1.10 | 3936 | 1.149 | 48.3 |
| 134.9* | 1.10 | 4345 | 1.149 | 58.9 |
| 134.9* | 1.10 | 4684 | 1.149 | 68.4 |
| 136.1 | 1.11 | 3326 | 1.147 | 34.7 |
| 139.2 | 1.10 | 3429 | 1.144 | 36.5 |
| 144.0 | 1.087 | 3488 | 1.139 | 37.2 |
| 148.3 | 1.075 | 3468 | 1.135 | 36.2 |

*see Table I.

**Values were obtained from smoothing $1/y_1$ vs $T$ data, see text.

where $\omega = 2\pi f_0$. Typical numbers are 128.1°C—3.7 cp, 131.5°—3.2 cp, 132.8°—4.5 cp, 134.7°—3.8 cp, 139.2°—3.4 cp. We remark that while the precision with which these numbers were determined was a few percent, the apparent accuracy was much poorer. The viscosity should vary smoothly with temperature but this was only approximately so. These results suggest that PAA was no stable enough for measurements using our cell design.

## DISCUSSION

The light scattering technique has proved to be an accurate, nonperturbing technique for the measurement of interfacial properties and certain volume properties such as the shear viscosity. The advantages as well as the precautions in applying the technique are thoroughly discussed in our recent papers on the instrumentation.[4,13]

The most interesting feature of the data we report is that of the large change in frequency and broadening of the spectral width of the 252 cm$^{-1}$ ripples observed at 134.9°C during the temperature jump experiment.

As we have mentioned, the temperature was changed from a set point by the application of a small increment of power to the cell heaters. This temperature increase amounted to about 0.2°C over approximately 10 min. When the set point was beyond ±1°C of the transition temperature the spectrum changed smoothly; $\omega$ and $\Gamma$ were what was expected for a continuous change in temperature from the set point. When the set point was 134.9°C, then the dramatic frequency change shown in Figure 3 was observed. We concluded that the frequency "jump" was associated with the nematic-isotropic phase transition.

There is no doubt of our observation of the large change we have documented.[2] However, we do not have enough data to decide whether our observations are unique to the particular PAA samples we used or whether the phenomenon is unique to PAA. Reasonable care was used in preparing the PAA sample for the experiment. Further, vacuum cleaning the surface was an effective method for removing surface contamination. With these points in mind we conclude that the phenomenon was not caused by contamination. It would be possible to observe an apparent increase in $\omega$ if $k_e$, as defined at the surface, was distorted by curvature of the liquid crystal surface. We demonstrated by direct measurement that the radius of curvature of the PAA liquid surface did not change with temperature through the range studied including the transition temperature. Temperature gradients can cause surface flows which in turn can shift the center frequency as well as change the width of the spectrum. This effect cannot be the cause of the change in the spectra at 134.9°C since the effect was observed only at that temperature and the shifts were much too large to be explained by any realistic estimate of the temperature gradients at the surface.

The mechanism for the observed variation in $\omega$ close to the transition temperature is not understood. One can build models based on coexistence of the isotropic and nematic phases during the temperature jump but it is not worthwhile to work out the details of such models until more information is obtained showing that the frequency variation we observed is intrinsic to the nematic-isotropic phase change. Obviously, other nematic liquid crystals should be studied. It will be important to collect such data as a function of $q$, the ripple wave number, in order to decide whether the effect is related to bending terms added to Eq. (1a) or a complicated constitutive relation representing elastic and viscosity coefficients in Eq. (1b). Moreover, a proper model for **P** will further complicate the dispersion relations.[3]

Table II shows the result of our attempt to calculate a best estimate of the surface tension over the temperature range of 128°C to 148°C. This table was constructed from smoothing the $1/Y_1$ data given in Table I giving less weight to data marked with * on the temperature column. Observe that, except for one number at 134.9°C, there is a scatter of only a few percent or less from a smooth line drawn through a $1/Y_1$ vs $T$ plot. The set of surface tension numbers was calculated using the definition of $Y_1$, $q = 252\ \mathrm{cm}^{-1}$, and the numbers given in Table II.

We remark that Langevin and Bouchiat[3] report that $\gamma = 38 \pm 4$ d/cm at 122°C with $q = 400\ \text{cm}^{-1}$. The numbers we give here are slightly larger than the PAA data reported by Krishnaswamy and Shashidhar[20] and therefore a few dynes per centimeter lower than other reports.[2] Our equilibrium surface tension numbers as a function of temperature on PAA scattered more than we had expected based on the work we have done with other liquids. This variation may have been due to the lack of really careful control of the vapor pressure[20] over the PAA in our measurements. Moreover, in retrospect, PAA does not appear to be the best liquid crystal material for the study of the surface tension change at the nematic-isotropic transition temperature. We found that it is volatile and in general rather difficult to handle.

The uncertainty in measuring $\Gamma$ because of the uncertainty in computing large instrumental corrections must be overcome. We believe that instrumental corrections of the order of a few percent can be obtained by a redesign of the optical arrangement. Obviously $\sigma_{\text{surf}}$ must be made larger, Eq. (9). However, there is a compromise that must be made since as the beam is expanded the signal-to-noise ratio becomes smaller. These factors are discussed in detail by Edwards *et al.*[4]

Also Lading[16] has shown how to minimize surface curvature effects as well as how to resolve $\eta(\mathbf{x})$ in Eq. 6, for certain ranges of surface density fluctuations. While resolving $\eta(\mathbf{x})$ is especially interesting for the case of monolayers spread on isotropic liquids, the function may be interesting to study for liquid crystal systems.

From a theoretical viewpoint it is hard to rationalize an apparent surface tension of 68 d/cm for a liquid crystal with an equilibrium surface tension of the order of 36 d/cm. If the measurements we report stand the test of confirmation then it is obvious that a more complicated model of the viscoelastic response must be used. Fortunately, the literature is rich in suggestions even though it is poor in experimental data. Moreover, the classical methods of measuring the surface tension, because they average out thermal fluctuations, may be incapable of detecting the phenomena we have reported herein.

Finally, the viscosity data deserve some comment. Our numbers are consistent with the one number reported by Langevin and Bouchiat[3] (3.6 ±0.4 cp at 122°C). We did not use an orienting magnetic field; it is likely that the PAA surfaces were unoriented with the director in the plane of the surface. As a result we expect $\mu_{\text{eff}} \sim \eta_1 + \eta_2 + \eta_3/8$ for such a situation. All we can say at this time is that it is reasonable to expect $\mu_{\text{eff}}$ to be larger than the numbers obtained by imposing a nonequilibrium velocity gradient field on the liquid crystal. Papoular and Rapini[9] also suggest a band broadening effect.

We believe that a study using the light scattering technique investigating a range of $q$ numbers at each temperature will produce enough data of high precision and accuracy so that viscoelastic coefficients including the surface tension and $\eta_1$, $\eta_2$ and $\eta_3$ can be determined. Moreover, questions we have raised about the various dispersion equations and the appropriateness of the constitutive relations for $\mathbf{P}$ and $\overline{\overline{\sigma}}$ can be studied in detail.

## Acknowledgment

The authors acknowledge the support from NASA-Marshall, NAS8-33015 and partial support from ONR as part of a SOR contract from CWRU. R. V. Edwards has contributed to this study in many ways: through many useful discussions, through many suggestions involving instrumental and theoretical questions, and his observation that only the ratio $\Gamma/\omega$ mattered led to a new and useful analysis scheme. We thank S. Rak for the radius of curvature measurements mentioned in this report.

## References

1. J. D. Parsons, *Mol. Cryst. Liq. Cryst.*, **31**, 79 (1975) and *J. de Phys.*, **37**, 1187 (1976); also see J. Murakami, *J. Phys. Soc., Japan*, **42**, 210 (1977) and C. A. Croxton, *Phys. Lett.*, **72A**, 136 (1979).
2. L. B. Shih, "Dynamic Light Scattering of Surface Fluctuations of a Nematic Liquid Crystal," Kent State University, Dissertation Abstracts International, **B**, **42**(8), 3285, (1982). Order #8202169.
3. D. Langevin and M. A. Bouchiat, *J. de Phys.*, **33**, 101 (1972), C1-77, and D. Langevin, *J. de Phys.*, **33**, 249 (1972).
4. R. V. Edwards, R. S. Sirohi, J. A. Mann, L. B. Shih and L. Lading, Applied Optics, **21**(19), 3555 (1982).
5. S. Hård, Y. Hamnerious and O. Nilsson, *J. Appl. Phys.*, **47**, 2433 (1976).
6. S. Hård and R. D. Neuman, *J. Coll. and Interface Sci.*, **83**, 315 (1981).
7. J. A. Mann, "Dynamic Surface Tension and Capillary Waves," in "Surface and Colloid Science," ed. E. Matijevic, Volume Editor R. J. Good, Plenum Press, New York, in press, 1983.
8. J. A. Mann and K. C. Prozio, "Capillarity: The Physical Nature of Fluid–Fluid Interfaces Including the Problem of Biomembrane Structures," Internation. Review of Sci. Phy. Chem. Series Two, Vol. 7, *Surface Chemistry and Coll.*, Ed. by M. Kerker, Butterworths, London, 1975.
9. M. Papoular and Rapini, *Solid State Communication*, **7**, 101 (1969); also see Reference 3.
10. L. Kramer, *J. Chem. Phys.*, **55**, 2097 (1971); also see C. Fan, *J. Coll. and Interface Sci.*, **44**, 369 (1973).
11. V. G. Levich, "Physicochemical Hydrodynamics," Prentice-Hall, Englewood Cliffs, N.J., 1962.
12. The original data are stored in tape files that are available from J. A. M. or L. B. S. in standard formats.
13. L. B. Shih, J. A. Mann and R. V. Edwards, "Surface Fluctuation Spectroscopy: A Novel Technique for Characterizing Liquid Interfaces," *Review of Scientific Inst.*, accepted March 3, 1983. Preprints are available.
14. D. Byrne and J. C. Earnshaw, *J. Colloid Interface Sci.*, **7**, 467 (1980).
15. Chatelain, *Bull. Soc. Fr. Miner. Crystallogr.*, **60** (1937) 280.

16. L. Lading, R. V. Edwards and J. A. Mann, "Fourier Optical Design of Surface Scattering Instrumentation," to be submitted to *J. Appl. Optics,* preprints available from J. A. M.
17. D. McQueen, *J. Phys. D* (Applied Physics) **6**, 2273 (1973).
18. R. S. Hansen and J. A. Mann, *J. Appl. Phys.*, **35**(1), 152 (1964).
19. M. A. Bouchiat and D. Langevin, *Phys. Letters,* **34A**, 331 (1971).
20. S. Krishnaswamy and R. Shashidhar, *Mol. Cryst. Liq. Cryst.*, **35**, 253 (1976).